

1 FA-SIFT study of the reactions of $\text{H}_3\text{O}^+(\text{H}_2\text{O})_n$ ($n=0,1,2$), NO^+ and
2 O_2^{++} with the terpenoid aldehydes citral, citronellal and myrtenal and
3 their alcohol analogues
4

5 C. Amelynck^{a,b,*}, B. Mees^{a,b}, N. Schoon^a, P. Bultinck^c
6

7 * Corresponding author. Tel. +32 2 373 03 90; Fax: +32 2 373 84 23.

8 *E-mail address:* crist.amelynck@aeronomie.be (C. Amelynck)

9 ^a Belgian Institute for Space Aeronomy, Ringlaan 3, B-1180 Brussels, Belgium

10 ^b Department of Analytical Chemistry, Ghent University, Krijgslaan 281, S12, B-9000 Ghent,
11 Belgium

12 ^c Department of Inorganic and Physical Chemistry, Ghent University, Krijgslaan 281, S3, B-
13 9000 Ghent, Belgium
14

15

16 Abstract
17

18 Biogenic volatile organic compounds (BVOCs) significantly contribute to atmospheric
19 chemistry, air quality and climate. On-line detection of these compounds can be performed by
20 Selected Ion Flow Tube – Mass Spectrometry (SIFT-MS), provided the rate constants and
21 product ion distributions of the underlying ion/molecule reactions are known. These
22 parameters are presented for the reactions of the SIFT-MS reagent ions $\text{H}_3\text{O}^+(\text{H}_2\text{O})_n$ ($n=0-2$),
23 NO^+ and O_2^{++} with the terpenoid aldehydes citral, citronellal and myrtenal and the terpenoid
24 alcohols citronellol and myrtenol. The experiments were performed at 295 K and 1.5 hPa in a
25 Flowing Afterglow Selected Ion Flow Tube (FA-SIFT) instrument. All studied reactions
26 proceed at the collision rate which is beneficial for the BVOC detection sensitivity. Non-
27 dissociative proton transfer, and elimination of a water molecule or simultaneous ejection of a
28 water molecule and C_4H_8 following protonation were observed as the major mechanisms for
29 most H_3O^+ reactions. Reactions of $\text{H}_3\text{O}^+(\text{H}_2\text{O})$ mainly proceeded by non-dissociative proton
30 transfer, possibly followed by ejection of a water molecule, whereas the main observed
31 mechanism for $\text{H}_3\text{O}^+(\text{H}_2\text{O})_2$ reactions was ligand switching followed by elimination of up to
32 three water molecules. Charge transfer occurred for all NO^+ reactions and was accompanied
33 by other major mechanisms such as hydride transfer and/or elimination of a water molecule
34 following charge transfer and/or ternary association. The O_2^{++} reactions generally resulted in
35 strong fragmentation. The product ion distributions suggest that selective detection of some

1 isomeric terpenoids might be possible. However, interference with simultaneously emitted
2 monoterpenes could be a problem.

3
4

5 Keywords: FA-SIFT, SIFT-MS, ion/molecule reactions, terpenoids, aldehydes, alcohols

6
7 1. Introduction

8

9 Terrestrial vegetation is a huge source of non-methane volatile organic compounds (VOCs),
10 also referred to as biogenic VOCs or BVOCs, of which terpene hydrocarbons and their
11 oxygenated derivatives (alcohols, aldehydes, ketones, ethers, acids, ...) constitute an important
12 fraction [1]. Because of their large emission rates and their high reactivity towards the main
13 atmospheric oxidants [2], these compounds play a major role in both gas-phase and particle-
14 phase atmospheric chemistry. They have a strong impact on the oxidative power of the
15 atmosphere by being a sink of OH[•] radicals (and thus influencing climate by affecting the
16 budget of atmospheric CH₄, a major greenhouse gas) and by influencing tropospheric O₃
17 levels. Furthermore, terpene oxidation products contribute to the formation and growth of
18 secondary organic aerosols, SOA, affecting air quality and climate as well [3].

19

20 Apart from influencing atmospheric chemistry, BVOC emissions are also believed to play a
21 role in plant functioning, e.g. by attracting pollinators or herbivore predators, deterring
22 herbivores, mediating plant-plant communication and by protecting the plant against
23 excessive heat or oxidative stress [4].

24

25 Whereas Gas Chromatography-Mass Spectrometry (GC-MS) can be considered the standard
26 technique to measure BVOCs, recently developed fast and sensitive on-line chemical
27 ionization mass spectrometry techniques, such as Selected Ion Flow Tube-Mass Spectrometry
28 (SIFT-MS) and Proton Transfer Reaction-Mass Spectrometry (PTR-MS), are steadily gaining
29 importance in BVOC research. Those techniques are based on chemical ionization of the
30 BVOCs by reaction with appropriate reactant ions (H₃O⁺, NO⁺ and O₂^{•+} in SIFT-MS, mainly
31 H₃O⁺ in PTR-MS), resulting in specific product ions. Details on the techniques can be found
32 in some excellent recent reviews ([5] for SIFT-MS, [6] for PTR-MS). Rate constants and
33 product ion distributions of the occurring reactant ion/BVOC reactions are required for
34 absolute BVOC quantification. In previous years, several systematic laboratory SIFT-MS and

1 PTR-MS ion/molecule reaction studies have been carried out in which these reaction
2 parameters were obtained for several terpenoid compounds (hemi-, mono- and sesquiterpenes,
3 terpenoid alcohols and some terpenoid ethers and esters) (reviewed in [7]). However, to the
4 best of our knowledge, no information is available yet on terpenoid aldehydes.

5
6 In this paper, calculated absolute rate constants, measured relative rate constants and
7 measured product ion distributions are presented for the reactions of the SIFT reagent ions
8 H_3O^+ , NO^+ and O_2^{++} with the monoterpene aldehydes citronellal and myrtenal, along with
9 their corresponding alcohols citronellol and myrtenol, respectively. Reactions with citral,
10 which is a mixture of neral and geranial, were studied as well. Ion/molecule reaction
11 parameters for the corresponding alcohols nerol and geraniol have been reported previously
12 [8]. When analyzing moist air samples by SIFT-MS, reactant H_3O^+ ions efficiently react with
13 H_2O molecules by ternary association to form higher-order proton hydrates. Therefore
14 reactions of the BVOCs with $\text{H}_3\text{O}^+(\text{H}_2\text{O})_n$ ($n=1,2$) have also been studied. The chemical
15 structure of the studied BVOCs is shown in Figure 1.

16
17 Citral, citronellol and citronellal are important constituents of the essential oils of several
18 plant species [9]. They have been identified as major components in the headspace of fresh
19 leaves of many citrus species [10,11] and are often used indoors as fragrance compounds in
20 air fresheners, cleaning products and as insect repellents. Since the gas-phase reactions of
21 citronellol with O_3 and OH [12], of citronellal with O_3 and OH [13] and of citral with O_3 [14]
22 were all found to be fast, not only the compounds themselves, but also their oxidation
23 products may well contribute to indoor pollution. All three compounds have also been
24 reported to possess antimicrobial effects [15].

25
26 Myrtenal was found to be emitted directly by loblolly pine (*Pinus taeda*) branches [16] and
27 the dependence of the myrtenal emission rates on environmental parameters (light intensity,
28 temperature, ...) was integrated in Version 2.1 of the Model for the Emissions of Gases and
29 Aerosols by Nature, MEGAN [17]. Both myrtenal and myrtenol have also recently been
30 identified in SOA from β -pinene ozonolysis [18], whereas myrtenol had been identified
31 previously as a minor gas phase product of β -pinene ozonolysis [19].

32
33
34

1

2 2. Experimental setup

3

4 2.1 Instrument

5

6 The gas phase ion/molecule reaction studies have been carried out in a Flowing Afterglow-
7 Selected Ion Flow Tube instrument (FA-SIFT) at 295 K and at a pressure of 1.5 hPa. Only a
8 brief description of the instrument will be given here, since it has been amply described in
9 previous papers [20,21]. Reactant ions are produced in a flowing afterglow reactor,
10 transported by an Ar buffer gas flow, sampled into a first vacuum chamber and pre-selected
11 according to their m/z ratio by a first quadrupole mass filter. Ions that are transmitted by the
12 filter are subsequently injected in the He buffer gas flow of the SIFT reactor by means of a
13 Venturi injector. At a fixed distance downstream of the reactant ion injection point, controlled
14 flows of the pure BVOC diluted in He are added to the main He buffer gas flow, resulting in
15 product ion formation. At the downstream end of the reactor, a small fraction of the ions is
16 sampled into a second vacuum chamber, analyzed according to their m/z ratio and
17 subsequently detected by a secondary electron multiplier with conversion dynode.

18

19 In previous ion/molecule reaction studies with this apparatus, product ion distributions have
20 been obtained by introducing the neutral reactant close to the mass spectrometer sampling
21 orifice in order to avoid corrections for the mass-dependent differential diffusion of the ions
22 to the reactor walls. In this study the terpenoid compounds were introduced via a ring-shaped
23 inlet which is also used for kinetic measurements and is located 27.8 cm upstream the
24 sampling point, corresponding with an experimentally determined reaction time of 2.8 ± 0.3
25 ms. Consequently much smaller BVOC concentrations are required in the SIFT reactor to
26 obtain the same decrease of the reactant ion signal due to reaction than when BVOCs are
27 introduced through the inlet near the sampling orifice. This firmly reduces the risk for
28 condensation of the low vapor pressure terpenoid aldehydes and alcohols in the pumps of the
29 instrument. The BVOC flow was dynamically diluted prior to entering the reactor by sending
30 a small He flow ($20 \text{ sccm} = 0.034 \text{ Pa m}^3 \text{ s}^{-1}$) over the surface of the pure liquid BVOC sample
31 stored in a glass vial, which was completely immersed in a thermostatted bath. Controlling the
32 BVOC flow was then accomplished by changing the pressure above the liquid through
33 variation of the conductance of a heated needle valve (333 K) between the liquid reservoir and
34 the SIFT reactor.

1

2 2.2 Methodology

3

4 2.2.1 Rate constants

5

6 Absolute ion/BVOC rate constant measurements with the SIFT apparatus require the
7 introduction of controlled and well-quantified BVOC flows in the reactor. In previous studies
8 (e.g. [22]), this was often accomplished by monitoring the pressure decrease in a volume-
9 calibrated glass bottle containing a dilute mixture of the BVOC in He with known mixing
10 ratio. The BVOC flow into the reactor was controlled by adjusting a heated needle valve
11 between the glass bottle and the reactor. However, for the compounds under study here,
12 attempts to produce stable static BVOC mixtures failed because of the stickiness of these
13 compounds.

14 A second method for introducing controlled and quantified BVOCs uses the same set-up as
15 described in paragraph 2.1. However, in order to quantify the BVOC flow with this method,
16 accurate values of the BVOC vapor pressure at the temperature of the glass reservoir are
17 required and this information is not available for the studied compounds.

18 Therefore absolute rate constant measurements could not be performed and we had to rely on
19 theoretical calculations of the H_3O^+ /BVOC collision rate constants to determine the reaction
20 rate constants of the other reactant ion species ($\text{H}_3\text{O}^+\cdot\text{H}_2\text{O}$, $\text{H}_3\text{O}^+(\text{H}_2\text{O})_2$, NO^+ , $\text{NO}^+\cdot\text{H}_2\text{O}$ and
21 O_2^+) with the BVOCs in a relative way. This is a sound way to do since many experimental
22 studies have shown that exothermic H_3O^+ /molecule reactions invariably proceed at the
23 collision rate [23].

24

25 2.2.1.1 Rate constant calculations

26

27 Absolute H_3O^+ /BVOC collision rate constants were calculated using the parameterized
28 equation of Su and Chesnavich [24,25], using values for the polarizability (α) and the electric
29 dipole moment (μ_D) of the BVOCs obtained from quantum chemical calculations (because of
30 lack of experimental data). As the required computed molecular parameters depend strongly
31 on the conformation, first a conformational analysis was performed for all molecules. Such a
32 detailed conformational analysis was carried out by combining a MMFF [26,27] random
33 search with a MM3/MM4 [28,29] stochastic search [30]. The minima that were found were
34 optimized at the B3LYP/6-31G(d,p) level and the Hessian was calculated to ensure that all

1 located stationary points were minima. All minima within an energy window of 16.75 kJ
2 mole⁻¹ were then re-optimized with the aug-cc-pVDZ basis set, and α and μ_D were calculated
3 for each minimum. All calculations were performed in the Ghent University scientific
4 computing environment using Gaussian09 [31]. Collision rate constants were calculated for
5 all individual conformations of a compound and subsequently Boltzmann-averaged using the
6 enthalpy to obtain a conformational population. The enthalpy was calculated at 295.15 K and
7 1.5 hPa via DFT using standard expressions [32]. Vibrational frequencies were scaled by a
8 factor 0.970 [33].

9
10 Calculations of H₃O⁺/VOC collision rate constants performed in previous studies using the
11 above-described methodology [8,34] resulted in a good agreement with experimental rate
12 constant values obtained with our SIFT instrument.

13

14 2.2.1.2 Relative rate constant measurements

15

16 The O₂^{•+}/BVOC rate constants were obtained relative to the H₃O⁺/BVOC rate constants by
17 simultaneously producing stable currents of both ion species in the flowing afterglow (FA)
18 reactor. This was accomplished by adding a small amount of water vapor to the Ar buffer gas
19 flow via a first reactant gas inlet in order to partially convert Ar⁺ ions, produced by electron
20 ionization using an emission current-controlled Thoria-coated Iridium filament, into a current
21 of H₃O⁺ ions and by adding a small flow of laboratory air via a second reactant gas inlet to
22 convert the remaining Ar⁺ ions to O₂^{•+} by reaction with O₂. The O₂^{•+} and H₃O⁺ ions were
23 sequentially transmitted by the selection quadrupole mass filter and introduced in the SIFT
24 reactor in the absence (I(O₂^{•+})₀ and I(H₃O⁺)₀) and in the presence of BVOC in the SIFT
25 reactor at different concentrations [M] (I(O₂^{•+})_M and I(H₃O⁺)_M). The rate constant ratio
26 k(O₂^{•+})/k(H₃O⁺) was obtained as the slope of the linear fit of ln(I(O₂^{•+})_M/ I(O₂^{•+})₀) versus
27 ln(I(H₃O⁺)_M/ I(H₃O⁺)₀).

28 In a similar way, O₂^{•+} and NO⁺ reactant ions were produced simultaneously in the flowing
29 afterglow reactor by simultaneous addition of small air and NO flows, allowing to infer the
30 rate constant ratio k(NO⁺)/k(O₂^{•+}).

31 The rate constant ratios k(H₃O⁺.H₂O)/k(H₃O⁺) and k(H₃O⁺.(H₂O)₂)/k(H₃O⁺.H₂O) were
32 obtained by adding appropriate amounts of water vapor to the FA reactor and pre-selecting
33 H₃O⁺.H₂O and H₃O⁺.(H₂O)₃ ions, respectively. Partial break-up of H₃O⁺.H₂O to H₃O⁺
34 upstream the reaction zone was accomplished by increasing the electric field in the vicinity of

1 the SIFT injection orifice. The ratio $k(\text{H}_3\text{O}^+.\text{H}_2\text{O})/k(\text{H}_3\text{O}^+)$ was obtained as the slope of
2 $\ln(I(\text{H}_3\text{O}^+.\text{H}_2\text{O})_M / I(\text{H}_3\text{O}^+.\text{H}_2\text{O})_0)$ versus $\ln(I(\text{H}_3\text{O}^+)_M / I(\text{H}_3\text{O}^+)_0)$.

3 In order to produce a stable and sufficiently intense $\text{H}_3\text{O}^+.\text{(H}_2\text{O)}_2$ current (resulting in > 1000
4 cps) in the SIFT reactor, $\text{H}_3\text{O}^+.\text{(H}_2\text{O)}_3$ ions were pre-selected and subjected to collision-
5 induced dissociation at the SIFT injector. By further increasing the electric field near the
6 orifice, break-up of $\text{H}_3\text{O}^+.\text{(H}_2\text{O)}_3$ ions led to the simultaneous and stable production of both
7 $\text{H}_3\text{O}^+.\text{(H}_2\text{O)}_2$ and $\text{H}_3\text{O}^+.\text{H}_2\text{O}$ ion currents in the SIFT reactor. The ratio
8 $k(\text{H}_3\text{O}^+.\text{(H}_2\text{O)}_2)/k(\text{H}_3\text{O}^+.\text{H}_2\text{O})$ was then obtained as the slope of $\ln(I(\text{H}_3\text{O}^+.\text{(H}_2\text{O)}_2)_M /$
9 $I(\text{H}_3\text{O}^+.\text{(H}_2\text{O)}_2)_0)$ versus $\ln(I(\text{H}_3\text{O}^+.\text{H}_2\text{O})_M / I(\text{H}_3\text{O}^+.\text{H}_2\text{O})_0)$.

10 The experimentally obtained rate constant ratios were then combined with the calculated
11 $\text{H}_3\text{O}^+/\text{BVOC}$ collision rate constant to obtain absolute rate constant values for the BVOC
12 reactions with the other reactant ions.

13 The rate constant ratio $k(\text{NO}^+.\text{H}_2\text{O})/k(\text{NO}^+)$ was obtained by injecting NO^+ ions into the
14 SIFT, adding controlled water vapor flows to the SIFT reactor and monitoring the NO^+ and
15 $\text{NO}^+.\text{H}_2\text{O}$ ion signals at different water vapor concentrations [35].

16

17 2.2.2 Product ion distributions

18

19 Product ions were identified by taking full mass spectra after which their ion signals were
20 recorded in the multiple ion monitoring mode, using at least three different BVOC
21 concentrations in the SIFT reactor. The product ion signals were subsequently corrected for
22 background contributions, mass discrimination and diffusion enhancement. Mass
23 discrimination of the instrument was obtained by sequentially injecting high purity currents of
24 single ion species X^+ into the SIFT and by simultaneously recording the corresponding
25 current (I) on the mass spectrometer inlet plate and the ion count rate (S) obtained with the
26 mass spectrometer. The X^+ species used for this purpose were, in addition to H_3O^+ , $\text{H}_3\text{O}^+.\text{H}_2\text{O}$
27 and SF_5^+ , primary and secondary product ions of proton hydrates with 1-penten-3-ol,
28 isopropanol and ethanol and encompassed m/z values between 19 and 155. The mass
29 discrimination factor (MDF) for these ion species was determined as the ratio $S/I(\text{H}_3\text{O}^+)$ to
30 $S/I(\text{X}^+)$. MDF values for the specific product ions of the studied ion/molecule reactions were
31 obtained from a polynomial fit through $S/I(\text{X}^+)$ versus $m/z(\text{X}^+)$. MDF-corrected product ion
32 signals were obtained by multiplying the background corrected ion signals by their
33 corresponding MDF value.

34

1 As already mentioned, diluted BVOC mixtures were introduced upstream of the mass
 2 spectrometer inlet and consequently differential diffusion of the precursor (S^+) and product
 3 (P^+) ions in the helium buffer gas had to be accounted for in order to obtain correct product
 4 ion distributions. This was accomplished by dividing the MDF-corrected product ion count
 5 rates by their respective diffusion enhancement factor, which is given by [36]:

$$DE(P^+) = \frac{e^{\frac{D_p(S^+) - D_p(P^+)}{\Lambda^2} \tau} - 1}{e^{\frac{D_p(S^+) - D_p(P^+)}{\Lambda^2} \tau}}$$

8
 9 In this formula, which is only valid for small concentrations of the reactant BVOC, Λ and τ
 10 are the characteristic length of the reactor and the reaction time, respectively. The former is
 11 obtained by the formula [37]:

$$\frac{1}{\Lambda^2} = \left(\frac{2.405}{r_0}\right)^2 + \left(\frac{\pi}{H}\right)^2$$

13
 14 with r_0 and H the radius of the reactor (2.0 cm) and the length of the reactor zone (27.8 cm),
 15 respectively, resulting in a value for Λ of 0.828 cm for our specific configuration.

16 The reaction time τ was determined experimentally by putting a short voltage pulse on the
 17 electrically insulated BVOC inlet and by measuring the arrival of the ion current perturbation
 18 on the mass spectrometer detector, the ion flight time in the mass spectrometer being
 19 negligible compared to the ion residence time between the BVOC inlet and the mass
 20 spectrometer inlet. This reaction time was found to be 2.8 ± 0.3 ms.

21 The free diffusion coefficient D_p of a specific ion species is related to its ion mobility K by
 22 the Nernst-Townsend-Einstein equation:

$$D_p = K \frac{k_b T}{q}$$

24
 25 with k_b , q and T the Boltzmann constant, the electrical charge of the ion and the temperature
 26 of the reactor, respectively. The ion mobility itself is calculated from standard ion mobility
 27 values taking into account the actual pressure and temperature in the reactor. Standard ion

1 mobility values for the different precursor and product ions in this work were obtained from a
2 fit through calculated K_0 values, reported by Dryahina et al. [38], versus m/z . For this fit only
3 the proton hydrates and organic ions mentioned in Table 1 of [38] were withheld.

4 5 2.3 Chemicals

6
7 All studied BVOCs were obtained from Sigma-Aldrich. The optically active compounds
8 (1R)-Myrtenal, (1R)-(-)-myrtenol, (R)-(+)-citronellal and (R)-(+)-beta-citronellol had a stated
9 purity of 98, 95, 98 and 98%, respectively. Citral is a racemic mixture of neral and geranial
10 and had a purity of 95%. The buffer gases He and Ar were obtained from Air Products and
11 both were 99.9997% pure.

12 13 3. Results and discussion

14 15 3.1 Rate constants

16
17 The calculated ion/BVOC collision rate constants are shown in Table 1, along with the
18 quantum chemically obtained electrical dipole moments and polarizabilities. Also shown are
19 the absolute reaction rate constants of $\text{H}_3\text{O}^+\cdot\text{H}_2\text{O}$, $\text{H}_3\text{O}^+(\text{H}_2\text{O})_2$, NO^+ , $\text{NO}^+\cdot\text{H}_2\text{O}$ and O_2^{*+} with
20 the studied BVOCs, obtained by using the calculated H_3O^+ /BVOC collision rate constants and
21 experimentally determined rate constant ratios $k(\text{O}_2^{*+})/k(\text{H}_3\text{O}^+)$, $k(\text{H}_3\text{O}^+\cdot\text{H}_2\text{O})/k(\text{H}_3\text{O}^+)$,
22 $k(\text{H}_3\text{O}^+(\text{H}_2\text{O})_2)/k(\text{H}_3\text{O}^+\cdot\text{H}_2\text{O})$, $k(\text{NO}^+)/k(\text{O}_2^{*+})$ and $k(\text{NO}^+\cdot\text{H}_2\text{O})/k(\text{NO}^+)$. The precision of the
23 first four rate constant ratios is 1%, resulting in a precision of less than 2% for the resulting
24 absolute rate constant. A precision of 3% was obtained for the latter rate constant ratio, which
25 was determined in a different way (see paragraph 2.2.1.2).

26 The calculated and experimentally obtained rate constants all show a good agreement,
27 indicating that all studied ion/molecule reactions proceed at the collision limit, which is
28 beneficial to the BVOC detection sensitivity by SIFT-MS.

29 30 3.2 Product ion distributions

31
32 The product ion distributions of $\text{H}_3\text{O}^+(\text{H}_2\text{O})_n$ ($n=0,1,2$), NO^+ and O_2^{*+} with citral, citronellal,
33 myrtenal, citronellol and myrtenol are gathered in Table 2. Only product ion species with
34 branching ratios higher than the impurity of the compound have been tabulated and isotopic

1 abundances were taken into account when calculating branching ratios. Tentative
 2 identification of the product ions is based on whether they form hydrates upon addition of
 3 water vapor to the SIFT reactor, as oxygenated hydrocarbon ions have a propensity to form
 4 hydrates, whereas pure hydrocarbon ions do not [39]. The relative error on individual
 5 branching ratios was found to be better than 3% for branching ratios above 80%, between 3
 6 and 7% for branching ratios between 50 and 80%, between 7 and 12% for branching ratios
 7 between 30 and 50% and varied between 6 and 24% for branching ratios between 2 and 30%.

8

9 3.2.1 Reactions with $\text{H}_3\text{O}^+(\text{H}_2\text{O})_n$ ($n=0,1,2$)

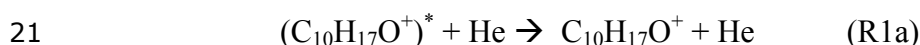
10

11 All studied $\text{H}_3\text{O}^+/\text{M}$ reactions were found to proceed by exothermic proton transfer, resulting
 12 in the nascent excited protonated molecule $(\text{MH}^+)^*$, which is either stabilized by collisions
 13 with a third body (He) or releases its excess energy by fragmentation. This is exemplified in
 14 the reaction of H_3O^+ with myrtenol (R1) for which the three major pathways are non-
 15 dissociative proton transfer (R1a), elimination of a water molecule following protonation
 16 (R1b), and ejection of $\text{C}_4\text{H}_{10}\text{O}$ following protonation (R1c). The latter pathway most probably
 17 involves simultaneous ejection of H_2O and C_4H_8 .

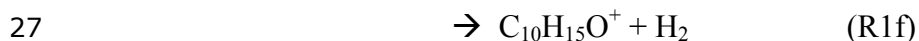
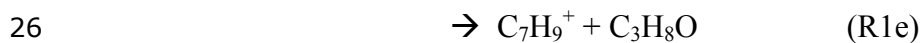
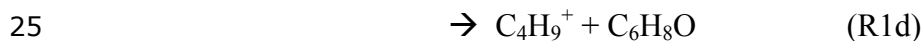
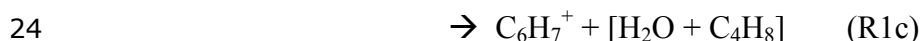
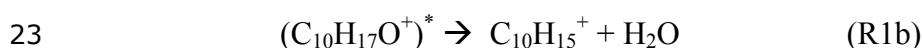
18



20



22



28

29 Several SIFT studies have shown that water elimination after protonation is a common
 30 mechanism for saturated and unsaturated, non-phenolic alcohols [8,34,39,40], strongly
 31 limiting the contribution of the non-dissociative proton transfer channel. The $\text{H}_3\text{O}^+/\text{myrtenol}$
 32 reaction follows this general observation, but this is not really the case for the
 33 $\text{H}_3\text{O}^+/\text{citronellol}$ reaction which has an MH^+ contribution of 49%.

34

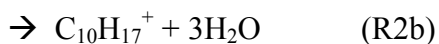
1 Water elimination following protonation is also an important process for citral and citronellal,
2 but is completely absent for myrtenal. This observation confirms the hypothesis, put forward
3 in previous systematic SIFT-MS studies on both saturated and unsaturated aldehydes [41,42],
4 that this process is restricted to those aldehydes which can form a cyclic six-membered
5 intermediate structure upon protonation (containing 4 Cs, O and H), which is clearly
6 impossible for the nascent excited protonated myrtenal molecule.

7
8 Several SIFT-MS and PTR-MS studies reported that the major product ions of
9 H_3O^+ /monoterpene ($\text{C}_{10}\text{H}_{16}$) reactions are the stabilized proton transfer product $\text{C}_{10}\text{H}_{17}^+$ (m/z
10 137) and a typical fragment C_6H_9^+ (m/z 81) due to ejection of C_4H_8 [22,43,44]. The same
11 difference in mass between the two major fragment ions is now encountered in the reactions
12 of three monoterpenoids (myrtenol (152 u), citronellol (156 u) and citronellal (154 u)) and
13 also in a previous study of the reactions of H_3O^+ with linalool (154 u), nerol (154 u) and
14 geraniol (154 u) [8], irrespective of the mass of the protonated terpenoid. This indicates that
15 the simultaneous occurrence of ions at m/z values x, x-18 and x-74 in mass spectra may point
16 to the presence of monoterpenoid alcohols and aldehydes of molecular mass x-1, but it is not a
17 general rule. Indeed, ejection of a C_4H_8 molecule from the major fragment (at m/z 135)
18 clearly does not take place in the case of the citral molecule for which major fragments at m/z
19 95 ($\text{C}_7\text{H}_{11}^+$) and at m/z 59 ($\text{C}_3\text{H}_7\text{O}^+$) have been observed.

20
21 Next to the three above-mentioned reaction channels, the H_3O^+ /myrtenol reaction also results
22 in the formation of fragment ions at m/z 57 (C_4H_9^+) and 93 (C_7H_9^+), and in ejection of a
23 hydrogen molecule following protonation. The latter process was also observed as a minor
24 channel in the reactions of H_3O^+ with the terpenoid alcohols verbenol [40] and geraniol [8].
25 The H_3O^+ /citronellol and H_3O^+ /citronellal reactions also led to a product ion at m/z 57
26 (C_4H_9^+) and 95 ($\text{C}_7\text{H}_{11}^+$), respectively. Small contributions (2-3%) of product ions at m/z 95
27 have also been reported for the acyclic terpenoid alcohols linalool, nerol and geraniol
28 ($\text{C}_{10}\text{H}_{18}\text{O}$, 154 u) [8], which are all isomers of citronellal.

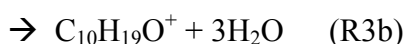
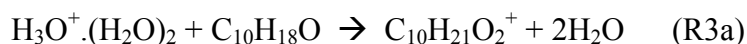
29
30 The reactions of $\text{H}_3\text{O}^+.\text{H}_2\text{O}$ with the studied compounds mainly proceed by non-dissociative
31 proton transfer (and even exclusively in the case of citronellol and myrtenal) and water
32 elimination following proton transfer, as exemplified by the reaction with citronellal (R2).





2
3 The lower exothermicity with respect to H_3O^+ reactions is sufficient to avoid additional
4 ejection of C_4H_8 . The $H_3O^+ \cdot H_2O$ /citral reaction, however, still results in product ions at m/z
5 95, but the channel leading to m/z 59 ions is no longer energetically accessible.

6
7 The reactions of $H_3O^+ \cdot (H_2O)_2$ proceed by ligand switching followed by elimination of up to 3
8 water molecules and is exemplified by the $H_3O^+ \cdot (H_2O)_2$ /citronellal reaction (R3).



13
14 Apart from the product ions that are mentioned in Table 2 and which have a contribution
15 larger than the impurity of the substance (5%), the $H_3O^+ \cdot (H_2O)_2$ /citral reaction also results in
16 product ions at m/z 95 ($C_7H_{11}^+$) and 135 ($C_{10}H_{15}^+$), with contributions of 4 and 3%,
17 respectively.

18 19 3.2.2 Reactions with NO^+

20
21 Charge transfer is the major reaction path for all NO^+ reactions indicating that the ionization
22 energy for all studied compounds must be lower than the one of NO , which is 9.26 eV. This
23 mechanism is especially dominant for citronellol, citronellal and myrtenol (79, 68 and 69%,
24 respectively). Elimination of a water molecule following charge transfer is only observed for
25 citronellal and citronellol. Similar to the H_3O^+ /myrtenal reaction, ejection of a water molecule
26 from the nascent excited myrtenal⁺* ion does not take place because a six-membered ring
27 structure, required for a McLafferty rearrangement [45], cannot form.

28
29 Myrtenal is also the only compound for which an association channel was observed. This
30 suggests that the difference in ionization energies of NO and myrtenal is probably sufficiently
31 small to allow charge delocalization around the $(NO \cdot myrtenal)^{+*}$ intermediate ion, hereby
32 increasing its lifetime and allowing collisional stabilization [42].

1 Hydride (H⁻) transfer, the second major pathway for myrtenal and citral, is a well-known
2 mechanism for reactions of NO⁺ with both alcohols [8,34,39,40] and aldehydes [41,46] and
3 results in HNO formation. This pathway is less important for citronellal (only 7%) and really
4 minor for the studied alcohols. Hydroxide transfer leading to HNO₂ formation, another
5 frequently observed mechanism for NO⁺/alcohol reactions in SIFT-MS conditions, does not
6 occur for any of the compounds in the present study.

7
8 Specific fragmentations (with contributions larger than 3%) were observed for myrtenol
9 (production of C₈H₁₂⁺ ions at m/z 108) and for citral (production of C₃H₇O⁺ and C₇H₁₀⁺ ions
10 at m/z 59 and 94, respectively).

11 12 3.2.3 Reactions with O₂⁺

13
14 Reactions of O₂⁺ with many BVOCs proceed via dissociative charge transfer and are
15 generally highly exothermic because of the high ionization energy of O₂ (12.07 eV). This
16 results in strong fragmentation of the nascent excited charge transfer product and
17 consequently in a large number of product ion species. This was also the case in the present
18 study. Whereas the contribution of the non-dissociative charge transfer channel varied
19 between 15 and 20% for the terpenoid aldehydes, it was found to be only 2% for the alcohols
20 (therefore not shown in Table 2). Other easily identifiable reaction mechanisms that took
21 place were elimination of a water molecule or of a methyl radical following charge transfer.
22 Most major fragment ions were also present in the electron ionization spectra of the molecules
23 [47].

24 25 3.2.4 Feasibility of isomer distinction

26
27 Several isomeric terpenoid alcohols and aldehydes, among others citronellal, geraniol, nerol
28 and linalool are co-emitted by fresh leaves of citrus species and their abundances are
29 generally strongly variety-dependent [10,11]. The present data, in combination with
30 previously reported data on the three alcohols [8], indicate an important difference in the
31 contribution of the collisionally stabilized protonated molecules to the corresponding product
32 ion distributions of their reaction with H₃O⁺. Whereas this contribution is 25% for citronellal,
33 it is only 4% for linalool and below 4% for nerol and geraniol. A rather similar difference was
34 found for the stabilized charge transfer product in the O₂⁺⁺ product ion distributions.

1 The feasibility of performing unambiguous concentration measurements of citronellal based
2 on the product ion signal at m/z 155 (protonated citronellal) using H_3O^+ reagent ions or at
3 m/z 154 (ionized citronellal) using O_2^{*+} reagent ions, however, will strongly depend on
4 individual mixing ratios of the different isomeric compounds. This will be even more the case
5 when using NO^+ reagent ions because of the very similar product ion distributions of the
6 reactions of citronellal, nerol and geraniol with NO^+ .

7
8 Moreover, it should be noted that, when measuring emissions from vegetation, these BVOCs
9 with a molar mass of 154 g/mol can be co-emitted with monoterpenes ($C_{10}H_{16}$). This may
10 result in important interferences for the detection of those terpenoid alcohols and aldehydes as
11 they have major product ions (at m/z 137 and 81) in common with the monoterpenes.

12 13 4. Conclusion

14
15 The rate constants and product ion distributions of the reactions of $H_3O^+(H_2O)_n$ ($n=0,1,2$),
16 NO^+ and O_2^{*+} with citral, citronellal, myrtenal, citronellol and myrtenol have been determined
17 in support of the detection of these biogenic terpenoid aldehydes and alcohols with SIFT-MS.
18 All reactions were found to occur at the collision limit, which favors detection sensitivity
19 provided that the contribution of the fingerprint product ions to the product ion distributions
20 of the specific BVOCs is sufficiently large.

21
22 The measurements show that both H_3O^+ and NO^+ reagent ions generally seem to be equally
23 well suited for quantification of the studied compounds. In Table 3, the contribution to the
24 product ion distribution of those product ions which can easily be related to the molecular
25 mass of the compound of interest is shown, i.e. those due to non-dissociative proton transfer,
26 water elimination following protonation and additional elimination of C_4H_8 in the case of
27 H_3O^+ reagent ions. The sum of those product ions makes up between 76 and 96% of all
28 product ions, except for citral for which this contribution is only 51%. Product ions resulting
29 from non-dissociative charge transfer, hydride transfer, water elimination following charge
30 transfer and termolecular association together constitute between 59 and 94% of the product
31 ions for the investigated BVOCs when using NO^+ reagent ions. Previously obtained SIFT-MS
32 data on terpenoid alcohols have also been gathered in Table 3, showing that the sum of the
33 product ions corresponding to the specified reaction channels for H_3O^+ and NO^+ constitutes a
34 major part of all product ions for these species as well. Moreover, the data in Table 3 reveal

1 once more that the simplistic notion often mentioned in the literature that the main product ion
2 for H_3O^+ reactions is the protonated molecule is an exception rather than the rule.

3
4 The product ion distributions of the isomeric compounds citronellal, nerol and geraniol
5 indicate that selective detection of citronellal using H_3O^+ or O_2^{*+} might be feasible, depending
6 on the differences in abundance of the different compounds in a mixture. However, care
7 should be taken when measuring terpenoid alcohols and aldehydes in the presence of
8 monoterpenes.

9

10 Acknowledgements

11

12 The computational resources (Stevin Supercomputer Infrastructure) and services used in this
13 work were provided by the VSC (Flemish Supercomputer Center), funded by Ghent
14 University, the Hercules Foundation and the Flemish Government – department EWI. P.
15 Bultinck acknowledges the Fund for Scientific Research - Flanders (FWO-Vlaanderen) and
16 the Research Board of Ghent University for continuous support.

17

18 References

19

- 20 [1] J. Kesselmeier, J. M. Staudt, *J. Atmos. Chem.* 33 (1999) 23-88.
- 21 [2] R. Atkinson, J. Arey, *Atmos. Environ.* 37 Supplement No. 2 (2003) S197-S219.
- 22 [3] G. Myhre, D. Shindell, F.-M. Bréon, W. Collins, J. Fuglestvedt, J. Huang, D. Koch, J.-F.
23 Lamarque, D. Lee, B. Mendoza, T. Nakajima, A. Robock, G. Stephens, T. Takemura, H.
24 Zhang, “Anthropogenic and Natural Radiative Forcing” in *Climate Change 2013: The*
25 *Physical Science Basis. Contribution of Working Group I to the Fifth Assessment Report of*
26 *the Intergovernmental Panel on Climate Change* [T.F. Stocker, D. Qin, G.-K. Plattner, M.
27 Tignor, S.K. Allen, J. Boschung, A. Nauels, Y. Xia, V. Bex and P.M. Midgley (eds.)],
28 Cambridge University Press, Cambridge, United Kingdom and New York, NY, USA, 2013.
- 29 [4] Ü Niinemets, *Trends in Plant Science* 15(3) (2010) 145-153.
- 30 [5] D. Smith, P. Španěl, *Mass Spectrom. Rev.* 24 (2005) 661-700.
- 31 [6] A.M. Ellis, C.A. Mayhew, *Proton Transfer Reaction Mass Spectrometry: Principles and*
32 *Applications*, John Wiley and Sons Ltd., Chichester, UK, 2014.
- 33 [7] C. Amelynck, N. Schoon, F. Dhooghe, *Current Analytical Chemistry* 9(4) (2013) 540-549.

- 1 [8] C. Amelynck, N. Schoon, T. Kuppens, P. Bultinck, E. Arijs, *Int. J. Mass Spectrom.* 247
2 (2005) 1-9.
- 3 [9] C. Sell, *A fragrant introduction to terpenoid chemistry*, The Royal Society of Chemistry,
4 2003.
- 5 [10] S.Y. Lin, S.F. Roan, C.L. Lee, I.Z. Chen, *Biosci. Biotechnol. Biochem.* 74(4) (2010)
6 806-811.
- 7 [11] M. Azam, Q. Jiang, B. Zhang, C. Xu, K. Chen, *Int. J. Mol. Sci.* 14 (2013) 17744-17766.
- 8 [12] J.E. Ham, S.P. Proper, J.R. Wells, *Atmos. Environ.* 40 (2006) 726-735.
- 9 [13] J.C. Harrison, J.E. Ham, J.R. Wells, *Atmos. Environ.* 41 (2007) 4482-4491.
- 10 [14] N. Fabíola Maria, M.C.C. Nunesa, P.A. Velosoa, P. de Pereira, J.B. de Andrade, *Atmos.*
11 *Environ.* 39(40) (2005) 7715-7730.
- 12 [15] A.A. Saddiq, S.A. Khayyat, *Pestic. Biochem. Phys.* 98 (2010) 89-93.
- 13 [16] C.D. Geron, R.R. Arnts, *Atmos. Environ.* 44 (2010) 4240-4251.
- 14 [17] A.B. Guenther, X. Jiang, C.L. Heald, T. Sakulyanontvittaya, T. Duhl, L.K. Emmons, X.
15 Wang, *Geosci. Model Dev.* 5 (2012) 1471-1492.
- 16 [18] T. Hohaus, D. Trimborn, A. Kiendler-Scharr, I. Gensch, W. Laumer, B. Kammer, S.
17 Andres, H. Boudries, K.A. Smith, D.R. Worsnop, J.T. Jayne, *Atmos. Meas. Tech.* 3 (2010)
18 1423-1436.
- 19 [19] M. Jaoui, R.M. Kamens, *J. Atmos. Chem.* 44 (2003) 259-297.
- 20 [20] F. Dhooghe, C. Amelynck, J. Rimetz-Planchon, N. Schoon, F. Vanhaecke, *Int. J. Mass*
21 *Spectrom.* 285(1-2) (2009) 31-41.
- 22 [21] F. Dhooghe, C. Amelynck, J. Rimetz-Planchon, N. Schoon, F. Vanhaecke, *Int. J. Mass*
23 *Spectrom.* 290(2-3) (2010) 106-112.
- 24 [22] N. Schoon, C. Amelynck, L. Vereecken, E. Arijs, *Int. J. Mass Spectrom.* 229 (2003) 231-
25 240.
- 26 [23] Y. Ikezoe, S. Matsuoka, M. Takebe, A. Viggiano, *Gas Phase Ion-Molecule Reaction Rate*
27 *Constants through 1986*, Maruzen, Tokyo, 1987.
- 28 [24] T. Su, W.J. Chesnavich, *J. Chem. Phys.* 76 (1982) 5183-5185.
- 29 [25] T. Su, *J. Chem. Phys.* 89 (1988) 5355.
- 30 [26] T.A. Halgren, *J. Comput. Chem.* 17 (1996) 490.
- 31 [27] T.A. Halgren, *J. Comput. Chem.* 17 (1996) 520.
- 32 [28] N.L. Allinger, Y.H. Yuh, J.H. Lii, *J. Am. Chem. Soc.* 111 (1989) 8551.
- 33 [29] N.L. Allinger, K.S. Chen, J.H. Lii, *J. Comput. Chem.* 17 (1996) 642.
- 34 [30] M.J. Saunders, *J. Am. Chem. Soc.* 109 (1987) 3150.

- 1 [31] M. J. Frisch, G. W. Trucks, H. B. Schlegel, G. E. Scuseria, M. A. Robb, J. R.
2 Cheeseman, G. Scalmani, V. Barone, B. Mennucci, G. A. Petersson, H. Nakatsuji, M.
3 Caricato, X. Li, H. P. Hratchian, A. F. Izmaylov, J. Bloino, G. Zheng, J. L. Sonnenberg, M.
4 Hada, M. Ehara, K. Toyota, R. Fukuda, J. Hasegawa, M. Ishida, T. Nakajima, Y. Honda, O.
5 Kitao, H. Nakai, T. Vreven, J. A. Montgomery, Jr., J. E. Peralta, F. Ogliaro, M. Bearpark, J. J.
6 Heyd, E. Brothers, K. N. Kudin, V. N. Staroverov, R. Kobayashi, J. Normand, K.
7 Raghavachari, A. Rendell, J. C. Burant, S. S. Iyengar, J. Tomasi, M. Cossi, N. Rega, J. M.
8 Millam, M. Klene, J. E. Knox, J. B. Cross, V. Bakken, C. Adamo, J. Jaramillo, R. Gomperts,
9 R. E. Stratmann, O. Yazyev, A. J. Austin, R. Cammi, C. Pomelli, J. W. Ochterski, R. L.
10 Martin, K. Morokuma, V. G. Zakrzewski, G. A. Voth, P. Salvador, J. J. Dannenberg, S.
11 Dapprich, A. D. Daniels, Ö. Farkas, J. B. Foresman, J. V. Ortiz, J. Cioslowski, and D. J. Fox,
12 Gaussian09, Revision D.01, Gaussian, Inc., Wallingford CT, 2009.
13
- 14 [32] D.A. McQuarrie, Statistical Thermodynamics, Harper and Row, New York, 1973.
- 15 [33] R.D. Johnson III (Ed.), NIST Standard Reference Database No. 101, Release May 11,
16 2005, <http://srdata.nist.gov//cccbdb>.
- 17 [34] N. Schoon, C. Amelynck, E. Debie, P. Bultinck, E. Arijs, *Int. J. Mass Spectrom.* 263
18 (2007) 127-136.
- 19 [35] E. Michel, N. Schoon, C. Amelynck, C. Guimbaud, V. Catoire, E. Arijs, *Int. J. Mass*
20 *Spectrom.* 244 (2005) 50-59.
- 21 [36] P. Španěl, D. Smith, *J. Am. Soc. Mass Spectrom.* 12 (2001) 863-872.
- 22 [37] E.A. Mason, E.W. McDaniel, *Transport properties of ions in gases*, John Wiley and
23 Sons, New York, 1988.
- 24 [38] K. Dryahina, P. Španěl, *Int. J. Mass Spectrom.* 244 (2005) 148-154.
- 25 [39] P. Španěl, D. Smith, *Int. J. Mass Spectrom.* 167/168 (1997) 375-388.
- 26 [40] G. Amadei, B.M. Ross, *Rapid Comm. Mass Spectrom.* 25 (2011) 162-168.
- 27 [41] P. Španěl, D. Smith, *Int. J. Mass Spectrom.* 165/166 (1997) 25-37.
- 28 [42] P. Španěl, J.M. Van Doren, D. Smith, *Int. J. Mass Spectrom.* 213 (2002) 163-176.
- 29 [43] T. Wang, P. Španěl, D. Smith, *Int. J. Mass Spectrom.* 228 (2003) 117-126.
- 30 [44] A. Tani, S. Hayward, A. Hansel, N. Hewitt, *Int. J. Mass Spectrom.* 239 (2004) 161-169.
- 31 [45] R.M. Smith, *Understanding mass spectra: a basic approach*, 2nd edition, John Wiley and
32 Sons, Inc., Hoboken, New Jersey, 2004.
- 33 [46] D. Smith, T.W.E. Chippendale, P. Španěl, *Rapid Commun. Mass Spectrom.* 28 (2014)
34 1917-1928.

1 [47] NIST Mass Spec Data Center, S.E. Stein, director, "Mass Spectra" in NIST Chemistry
2 WebBook, NIST Standard Reference Database Number 69, Eds. P.J. Linstrom and W.G.
3 Mallard, National Institute of Standards and Technology, Gaithersburg MD, 20899,
4 <http://webbook.nist.gov>, (retrieved October 20, 2014).

5

6 Figure captions

7

8 Figure 1: structures of studied terpenoid aldehydes and alcohols

9

10

11

compound	μ_D (Debye)	α (\AA^3)	$k_{\text{exp}} [k_c] (10^{-9} \text{ cm}^3 \text{ s}^{-1} \text{ molecule}^{-1})$					
			H_3O^+	$\text{H}_3\text{O}^+ \cdot \text{H}_2\text{O}$	$\text{H}_3\text{O}^+ \cdot (\text{H}_2\text{O})_2$	NO^+	$\text{NO}^+ \cdot \text{H}_2\text{O}$	O_2^{++}
citral	4.39	20.3	[5.9]	4.5 [4.4]	3.8 [3.8]	5.1 [4.8]		4.9 [4.7]
citronellal	2.88	19.6	[4.3]	3.3 [3.2]	2.9 [2.8]	3.6 [3.5]	3.2 [2.9]	3.5 [3.4]
citronellol	1.62	16.6	[3.1]	2.2 [2.3]	1.8 [2.0]	2.5 [2.5]	2.3 [2.1]	2.5 [2.4]
myrtenal	3.91	17.8	[5.3]	3.8 [4.0]	3.2 [3.4]	4.4 [4.3]	4.0 [3.6]	4.3 [4.2]
myrtenol	1.71	15.1	[3.0]	2.3 [2.3]	1.9 [2.0]	2.5 [2.5]	2.4 [2.1]	2.5 [2.4]

Table 1: Experimentally determined reaction rate constants (k_{exp}) and calculated collision rate constants (k_c) for the studied ion/molecule reactions. Dipole moments μ_D and polarizabilities α are obtained from quantum chemical calculations.

Molecule formula mass (u)	H ₃ O ⁺			H ₃ O ⁺ .H ₂ O			H ₃ O ⁺ .(H ₂ O) ₂			NO ⁺			O ₂ ⁺⁺		
	m/z	formula	%	m/z	formula	%	m/z	formula	%	m/z	formula	%	m/z	formula	%
citral	59	C ₃ H ₇ O ⁺	11	95	C ₇ H ₁₁ ⁺	38	153	C ₁₀ H ₁₇ O ⁺	22	59	C ₃ H ₇ O ⁺	8	59	C ₃ H ₇ O ⁺	8
C ₁₀ H ₁₆ O	95	C ₇ H ₁₁ ⁺	27	135	C ₁₀ H ₁₅ ⁺	12	171	C ₁₀ H ₁₉ O ₂ ⁺	70	94	C ₇ H ₁₀ ⁺⁺	20	69	C ₅ H ₉ ⁺	13
152	135	C ₁₀ H ₁₅ ⁺	10	153	C ₁₀ H ₁₇ O ⁺	49	others		8	151	C ₁₀ H ₁₅ O ⁺	28	84	C ₅ H ₈ O ⁺⁺	8
	153	C ₁₀ H ₁₇ O ⁺	41	Others		1				152	C ₁₀ H ₁₆ O ⁺⁺	31	94	C ₇ H ₁₀ ⁺⁺	15
	others		11							others		13	109	C ₈ H ₁₃ ⁺	7
													152	C ₁₀ H ₁₆ O ⁺⁺	15
													others		34
citronellal	81	C ₆ H ₉ ⁺	23	137	C ₁₀ H ₁₇ ⁺	35	137	C ₁₀ H ₁₇ ⁺	7	111	C ₇ H ₁₁ O ⁺	3	84	C ₅ H ₈ O ⁺⁺	5
C ₁₀ H ₁₈ O	95	C ₇ H ₁₁ ⁺	4	155	C ₁₀ H ₁₉ O ⁺	64	155	C ₁₀ H ₁₉ O ⁺	29	112	C ₇ H ₁₂ O ⁺⁺	3	98	C ₆ H ₁₀ O ⁺⁺	4
154	137	C ₁₀ H ₁₇ ⁺	44	others		1	173	C ₁₀ H ₂₁ O ₂ ⁺	64	136	C ₁₀ H ₁₆ ⁺⁺	13	109	C ₈ H ₁₃ ⁺	3
	155	C ₁₀ H ₁₉ O ⁺	25							153	C ₁₀ H ₁₇ O ⁺	7	110	C ₈ H ₁₄ ⁺⁺	13
	others		4							154	C ₁₀ H ₁₈ O ⁺⁺	68	111	C ₇ H ₁₁ O ⁺	8
										others		6	112	C ₇ H ₁₂ O ⁺⁺	5
													121	C ₉ H ₁₃ ⁺	7
													136	C ₁₀ H ₁₆ ⁺⁺	10
													139	C ₉ H ₁₅ O ⁺	4
													154	C ₁₀ H ₁₈ O ⁺⁺	20
													others		21
citronellol	57	C ₄ H ₉ ⁺	8	157	C ₁₀ H ₂₁ O ⁺	100	157	C ₁₀ H ₂₁ O ⁺	70	137	C ₁₀ H ₁₇ ⁺	3	68	C ₅ H ₈ ⁺⁺	3
C ₁₀ H ₂₀ O	83	C ₆ H ₁₁ ⁺	16				175	C ₁₀ H ₂₃ O ₂ ⁺	30	138	C ₁₀ H ₁₈ ⁺⁺	12	69	C ₅ H ₉ ⁺	3
156	139	C ₁₀ H ₁₉ ⁺	17							155	C ₁₀ H ₁₉ O ⁺	3	71	C ₄ H ₇ O ⁺	8
	157	C ₁₀ H ₂₁ O ⁺	49							156	C ₁₀ H ₂₀ O ⁺⁺	79	81	C ₆ H ₉ ⁺	12
	others		10							others		3	82	C ₆ H ₁₀ ⁺⁺	16
													95	C ₇ H ₁₁ ⁺	9
													96	C ₇ H ₁₂ ⁺⁺	3

													109	C ₈ H ₁₃ ⁺	5
													110	C ₈ H ₁₄ ⁺⁺	3
													123	C ₉ H ₁₅ ⁺	12
													138	C ₁₀ H ₁₈ ⁺⁺	7
													others		19
myrtenal	151	C ₁₀ H ₁₅ O ⁺	96	151	C ₁₀ H ₁₅ O ⁺	99	151	C ₁₀ H ₁₅ O ⁺	23	107	C ₇ H ₇ O ⁺	3	79	C ₆ H ₇ ⁺	11
C ₁₀ H ₁₄ O	others		4	others		1	169	C ₁₀ H ₁₇ O ₂ ⁺	75	149	C ₁₀ H ₁₃ O ⁺	28	106	C ₈ H ₁₀ ⁺⁺	23
150							others		2	150	C ₁₀ H ₁₄ O ⁺⁺	35	107	C ₇ H ₇ O ⁺	18
										180	C ₁₀ H ₁₄ NO ₂ ⁺	18	108	C ₇ H ₈ O ⁺⁺	15
										others		16	135	C ₉ H ₁₁ O ⁺	2
													150	C ₁₀ H ₁₄ O ⁺⁺	17
													Others		14
myrtenol	57	C ₄ H ₉ ⁺	5	135	C ₁₀ H ₁₅ ⁺	78	135	C ₁₀ H ₁₅ ⁺	85	108	C ₈ H ₁₂ ⁺⁺	17	79	C ₆ H ₇ ⁺	35
C ₁₀ H ₁₆ O	79	C ₆ H ₇ ⁺	16	151	C ₁₀ H ₁₅ O ⁺	5	189	C ₁₀ H ₂₁ O ₃ ⁺	7	152	C ₁₀ H ₁₆ O ⁺⁺	69	91	C ₇ H ₇ ⁺	8
152	93	C ₇ H ₉ ⁺	5	153	C ₁₀ H ₁₇ O ⁺	5	others		8	others		14	108	C ₈ H ₁₂ ⁺⁺	17
	135	C ₁₀ H ₁₅ ⁺	53	others		12							121	C ₉ H ₁₃ ⁺	7
	151	C ₁₀ H ₁₅ O ⁺	5										others		33
	153	C ₁₀ H ₁₇ O ⁺	7												
	others		9												

Table 2: Product ion distributions of the reactions of H₃O⁺, H₃O⁺.H₂O, H₃O⁺.(H₂O)₂, NO⁺ and O₂⁺⁺ with terpenoid aldehydes and alcohols at 1.5 hPa and 295 K.

Molecule	M (g/mol)	characterization	H_3O^+				NO^+					O_2^{*+}
			MH^+	$(\text{MH}-\text{H}_2\text{O})^+$	$(\text{MH}-\text{H}_2\text{O}-\text{C}_4\text{H}_8)^+$	sum	M^{*+}	$(\text{M}-\text{H})^+$	$(\text{M}-\text{H}_2\text{O})^{*+}$	$(\text{MNO})^+$	sum	M^{*+}
Citronellal ^a	154	AC/NS	25	44	23	92	68	7	13	-	88	20
Citral ^a	152	BC/NS	41	10	-	51	31	28	-	-	59	15
Myrtenal ^a	150	BC/NS	96	-	-	96	35	28	-	18	81	17
Citronellol ^a	156	AC/NS	49	17	16	82	79	3	12	-	94	-
Borneol ^b	154	BC/S	-	100	-	100	33	67	-	-	100	13
Isoborneol ^b	154	BC/S	-	100	-	100	42	58	-	-	100	7
Linalool ^{b,c}	154	AC/NS	4	56	30	90	5	-	53	-	58	-
Geraniol ^c	154	AC/NS	3	62	23	88	37	5	22	-	64	2
Nerol ^c	154	AC/NS	-	64	31	95	54	-	22	-	76	4
Menthol ^d	154	MC/S	-	100	-	100	-	50	-	-	50	-
Verbenol ^b	152	BC/NS	3	42	-	45	2	-	7	25	34	-
Myrtenol ^a	152	BC/NS	7	53	16	76	69	-	-	-	69	-
Carvacrol ^b	150	PH	100	-	-	100	69	13	18	-	100	22
Thymol ^b	150	PH	100	-	-	100	100	-	-	-	100	49

Table 3: Contributions of the MH^+ , $(\text{MH}-\text{H}_2\text{O})^+$ and $(\text{MH}-\text{H}_2\text{O}-\text{C}_4\text{H}_8)^+$ reaction pathways, of the M^{*+} , $(\text{M}-\text{H})^+$ and $(\text{M}-\text{H}_2\text{O})^+$ reaction pathways and of the M^{*+} reaction pathway to the product ion distributions of the reactions of H_3O^+ , NO^+ and O_2^{*+} , respectively, with terpenoid aldehydes

and alcohols that have been studied by SIFT-MS. ^a this work, ^b [40], ^c [8], ^d [39], AC: acyclic, MC: monocyclic, BC: bicyclic, S: saturated, NS: non-saturated, PH: phenolic